# Robust Anatomy Recognition Approach for Automated Scan Planning of Spine MRI Examinations

**H. S. Heese[1], D. Bystrov[1], V. Pekar[2], S. P. Dries[1], R. Grewer[1], C. J. den Harder[3], R. Bergmans[3], A. W. Simonetti[3], and A. M. van Muiswinkel[3]**

[1]Philips Research Europe, Hamburg, Germany, [2]Philips Research North America, Markham, ON, Canada, [3]Philips Medical Systems, Best, Netherlands

## Introduction

Automated scan planning (ASP) has been successfully applied to various anatomies[1-6], superseding the extremely tedious and time-consuming task of manually planning diagnostic MRI scan volumes. Thus ASP improves the MRI acquisition workflow and yields consistent image orientations for subsequent diagnostic scans. Especially in spine examinations, intra-image, intra- and inter-subject variability hamper anatomy recognition, which is the key prerequisite. Extending on previous work[1], an improved anatomy recognition approach to an ASP method for MRI examinations of the lumbar and cervical section of the human spine is proposed. The main contributions of this work are improved filtering techniques, a multi-seed strategy for the detection of intervertebral discs, and the use of a statistical model for labelling the detected section of the spine column.

## Methods

As reported previously[1,2,3], the proposed ASP method consists of two main building blocks – a geometry learning / planning part, and an anatomy recognition part, which is carried out on a dedicated 3-D T1-weighted fast field echo (FFE) survey scan. The improved anatomy recognition successively performs three major processing steps.

i) Disc Candidate Detection: In the first step, candidate points and orientations for the visible intervertebral discs are computed by downsampling and filtering the survey for bright, line-like structures on sagittal 2-D slices. Disc candidates are then computed from the morphologically cleaned filter response as the centres of clusters that are derived via 3-D connected component analysis. The smallest principal component of each cluster is used as an approximation to the upward normal of the disc candidate. Whereas previously filtering was carried out for horizontal structures with an unspecifically wide range for the normal direction, images are now filtered for angulated line-like structures in different orientations in combination with a more confined variability range for the normal in order to increase sensitivity of the method.

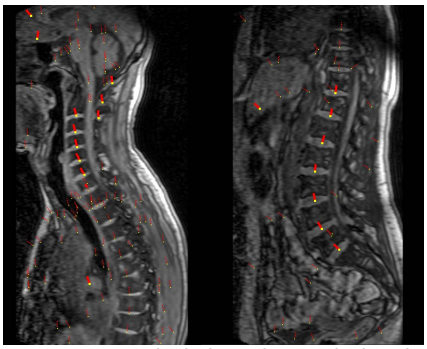

**FIGURE 1**: Sagittal view of a cervical and a lumbar survey image. Results of candidate detection step with improved filtering are indicated by yellow dots (centre of disc candidate) and red lines (upward normal of the disc candidate). Thinner dots and lines belong to other slices of the volume.

ii) Spine Column Selection: In the second step, the detected disc candidates are grouped in one-dimensional chains in a bottom-up, multi-seed fashion. Based on positional and directional information from the first step, each disc candidate predicts the position of its neighbouring upper, respectively lower, intervertebral disc from a projected, median-filtered one-dimensional intensity profile. Given these predictions, two candidates are said to form a strong connection if one is the nearest neighbour to the upper, respectively lower, prediction of the other, and vice versa. This defines a symmetric relation of adjacency on the set of candidates. Additional constraints on minimal and maximal distances between candidates are applied to avoid neglecting dim discs and to exclude bright spots in the vertebral bodies. One-dimensional chains are built from consecutive strong connections and the longest chain is selected as the set of disc candidates representing the spine column. Possible failed detections of disc candidates from the first step can be recovered by iteratively extending the selected candidate chain both in the upward and downward direction.

iii) Spine Labelling: In the third step, the obtained chain of candidates is labelled. For cervical images, the labelling starts above the uppermost candidate with vertebrae C1/2 and proceeds downward until the lower end of the chain is reached. For lumbar images, the lumbosacral transition of the spine column is detected by fitting a statistical model for the lower lumbar part of the spine column to the chain of candidates. This procedure allows for shortening the chain again by excluding implausible combinations of candidates, accounting for the possibility of the chain containing false candidates at its lower end. Then the labelling proceeds upward from vertebra S1 similar to the cervical case.

## Results

The method was evaluated on 38 cervical and 52 lumbar survey images (60 volunteer images, 30 clinical examinations) that have been acquired on Philips Panorama 1T open, or Philips Achieva 1.5T and 3T scanners. Sensitivity of the first step was tested against manually annotated ground truth resulting in a detection rate of 98.1% for the intervertebral discs C2/C3 to Th1/Th2, and respectively 98.6% for the intervertebral discs Th11/Th12 to L5/S1. The average amount of detected candidates was 131 for cervical images and 43 for lumbar images (see Fig. 1 for examples of Disc Candidate Detection). Spine Column Selection from these candidates successfully yielded chains corresponding to intervertebral discs in 100% of the cases. Labelling of the spine column was correct in 45 cases for lumbar images, while in 7 cases the labelling was shifted by either one or two vertebrae. For cervical images, 34 cases with correct labelling and 4 cases with the labelling being shifted were observed. (see Fig. 2 for examples of Spine Labelling).

## Discussion / Conclusions

Results reveal improved performance of both disc candidate detection and spine labelling compared to earlier work[1]. It can be seen (see Fig. 1) that orientations of the visible intervertebral discs vary widely even within the same section of the spine column, with the upward normals being on average rotated slightly anterior in cervical images, and often rotated posterior in lumbar images. Applied filtering accounts for both variability and average deviation from a straight upward direction yielding increased directional sensitivity. Thus, robustness of the entire method is improved through more reliable estimation of the normal direction of the discs (see Fig. 2). Multi-seed chain building has proven to be more robust than previous propagation-based methods in presence of 'missing' candidates or corrupted normal directions. Improved detection rates for the lumbosacral transition resulted in a positive effect on correctness of spine labelling. With overall computation time of about 10s (including planning) the algorithm proved to be competitive for use in daily clinical routine.

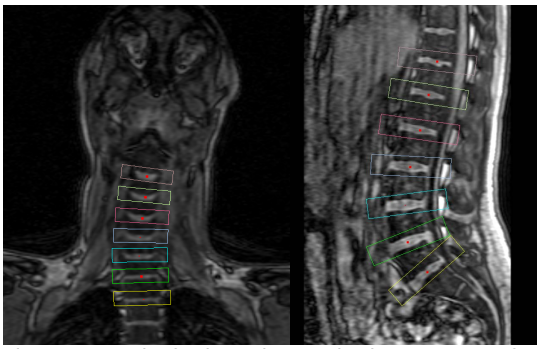

Figure 2: Result of spine column selection – centres of selected discs are shown as red dots in coronal (cervical) or sagittal (lumbar) orientation surrounded by coloured boxes that indicate detected disc orientation.

## References

1. Pekar V, et al.: Proc. MICCAI, 2007
2. Young S, et al.: Proc. SPIE Med. Imag.: 61441M, 2006
3. Bystrov D, et al.: Proc. SPIE Med. Imag.: 65902Z, 2007
4. Lelieveldt R, et al.: Radiology **221**: 537, 2001
5. Peng Z, et al.: IEEE-EMBS: 2527, 2005
6. Weiss K, et al.: Radiology **239**(1): 255, 2006